Structural, electronic, and optical absorption properties of orthorhombic $CaSnO_3$ through *ab initio* calculations

2007 J. Phys.: Condens. Matter 19 106214

(http://iopscience.iop.org/0953-8984/19/10/106214)

IOP PUBLISHING JOURNAL OF PHYSICS: CONDENSED MATTER

J. Phys.: Condens. Matter **19** (2007) 106214 (9pp) doi:10.1088/0953-8984/19/10/106214

Structural, electronic, and optical absorption properties of orthorhombic $CaSnO_3$ through *ab initio* calculations

J M Henriques[1], E W S Caetano[2,4], V N Freire[3], J A P da Costa[3] and E L Albuquerque[1]

[1] Departamento de Física Teórica e Experimental, Universidade Federal do Rio Grande do Norte, 59072-900 Natal, Rio Grande do Norte, Brazil
[2] Centro Federal de Educação Tecnológica do Ceará, Avenida 13 de Maio, 2081, Benfica, 60040-531 Fortaleza, Ceará, Brazil
[3] Departamento de Física, Universidade Federal do Ceará, Centro de Ciências, Caixa Postal 6030, Campus do Pici, 60455-760 Fortaleza, Ceará, Brazil

E-mail: ewcaetano@gmail.com

Received 15 October 2006, in final form 14 December 2006
Published 23 February 2007
Online at stacks.iop.org/JPhysCM/19/106214

Abstract

Density functional theory *ab initio* calculations of the structural parameters, electronic structure, carriers' effective masses, and optical absorption of orthorhombic $CaSnO_3$ were performed within the local density and generalized gradient approximations, LDA and GGA, respectively. A good agreement between the calculated lattice parameters and experimental results was obtained, and a direct energy gap of 1.95 eV (2.92 eV) is estimated in the GGA (LDA) for orthorhombic $CaSnO_3$. The computed carriers' effective masses are small and practically isotropic for electrons, allowing us to suggest that direct gap orthorhombic $CaSnO_3$ is a semiconductor with potential for optoelectronic applications. The optical absorption increases for photon energies larger than 7.0 eV due to the appearance of transitions involving O 2p valence states and Ca 3d conduction states.

1. Introduction

Stannate $CaSnO_3$ has attracted considerable attention in recent years. Difficulties of recovering samples of $CaSiO_3$ perovskite under ambient conditions (between 6% and 12% of the Earth's lower mantle weight are constituted of $CaSiO_3$ perovskite under pressures varying from 24 to 136 GPa) cause systematic relationships between the measured elasticity of other oxide perovskites (e.g. $CaSnO_3$) and their physical and structural properties to be

[4] Address for correspondence: Departamento de Física, Universidade Federal do Ceará, Centro de Ciências, Caixa Postal 6030, Campus do Pici, 60455-760 Fortaleza, Ceará, Brazil.

employed in order to predict the $CaSiO_3$ perovskite properties by extrapolation [1]. $CaSnO_3$ is also an interesting material with promising technological applications as: a high-capacity anode material for Li-ion batteries [2]; a phosphorescent material for traffic signs, interior decoration, and light sources ($CaSnO_3$:Tb has an afterglow of four hours after irradiation by 254 nm light [3], and the $CaSnO_3$:Eu^{3+} emission spectrum is dominated by the red $^5D_o \rightarrow {}^7F_2$ transition at 614 nm [4]); a capacitor component, since sintered $CaSnO_3$ samples are invariant over several decades of frequency [5]; a transparent conducting oxide (TOC) candidate for a wide variety of applications including flat panel displays, energy-efficient windows and anti-static coatings [6].

$CaSnO_3$ presents two crystalline forms: an ordered ilmenite phase with hexagonal and rhombohedral unit-cell parameters $a = 5.487(1)$ Å, $c = 15.287(6)$ Å, $Z = 6$ and $a = 6.000(2)$ Å, $\alpha = 54.42(3)^\circ$, $Z = 2$, respectively [7]; and an orthorhombic phase with perovskite structure, space group $Pbnm$, with $a = 5.5142(2)$ Å, $b = 5.6634(2)$ Å, $c = 7.88162(17)$ Å [8, 9]. An electronic structure study of $CaSnO_3$ ilmenite was performed recently with the linear muffin-tin orbital method and the atomic sphere approximation including the combined correction [6]. The Perdew–Wang generalized gradient approximation (GGA) was employed to treat the effects of exchange and correlation. A 4.0 eV direct energy gap was obtained for ilmenite $CaSnO_3$, which is in good agreement with the measured value of 4.4 eV [6]. To the knowledge of the authors, there is no similar first-principles calculation for the orthorhombic $CaSnO_3$ perovskite, which is the most used phase for technological applications. In this work, *ab initio* quantum mechanical calculations of the structural, electronic, and optical absorption properties of $CaSnO_3$ orthorhombic are performed for the first time within the realms of density functional theory [10, 11], putting forward estimates for the effective masses for electrons and holes, as well as optical absorption properties.

2. Theoretical methodology and structural results

The $CaSnO_3$ perovskite of orthorhombic symmetry $Pbnm$ has tilted and distorted SnO_6 octahedra with average Sn–O–Sn tilt angles of 147° [8], as shown in figure 1. The $CaSnO_3$ perovskite unit-cell parameters and atomic positions measured by x-ray diffraction [8, 9] are the starting point for our *ab initio* geometry optimization. The calculations were carried out using the CASTEP code [12] within the framework of the density functional theory (DFT) [10, 11] adopting a plane-wave basis and ultrasoft Vanderbilt pseudopotentials [13]. Exchange–correlation potentials were considered in both the local density and generalized gradient approximations, LDA and GGA, respectively. In the former, the exchange–correlation energy depends only on the electronic density at a given point [14]. In the latter, not only the electronic density but also its gradient is considered to account for the nonhomogeneity of the true electron density. The generalized gradient approximation (GGA) in many cases considerably improves the description of bonding with respect to the pure LDA, with some increase of computational cost. However, as we will see in this paper, the unit-cell parameters predicted in the LDA framework for orthorhombic $CaSnO_3$ are in better agreement with experiment. For the LDA exchange–correlation energy we use the CA–PZ parametrization (Ceperley and Alder [15]–Perdew and Zunger [16]), while for the GGA approach our choice was to adopt the Perdew–Burke–Ernzerhof exchange and correlation terms [17].

The valence shells for the ultrasoft pseudopotentials were Ca $3s^2 3p^6 4s^2$, Sn $5s^2 5p^2$, and O $2s^2 2p^4$. The oxygen pseudopotential was generated on-the-fly with a plane-wave cutoff energy of 550 eV. The Monkhorst–Pack scheme for integration in the Brillouin zone [18, 19] with a $5 \times 4 \times 6$ grid was adopted. After optimization, the electronic structure and optical absorption were calculated. The density of states (DOS) was computed by means of a scheme

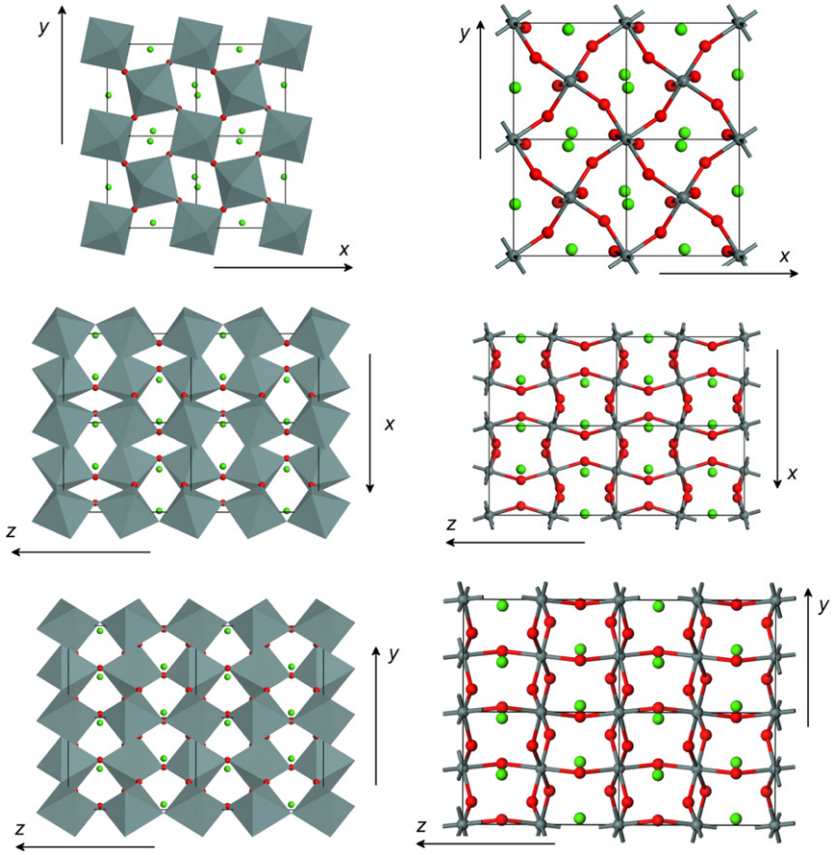

Figure 1. Orthorhombic $CaSnO_3$ crystal: different views of a $2 \times 2 \times 2$ supercell.
(This figure is in colour only in the electronic version)

developed by Ackland [20], while the partial density of states (PDOS) calculation was based on a Mulliken population analysis with the relative contribution of each atom [21, 22].

Geometry optimization was carried out using the Broyden–Fletcher–Goldfarb–Shannon algorithm [23], enabling us to obtain the best unit-cell parameters (lattice parameters, unit-cell angles, internal atomic coordinates). A 600 eV energy cutoff for the plane-wave basis set and a tolerance of 5×10^{-7} eV/atom for the self-consistent field calculations was adopted. In order to find the lowest energy structure of $CaSnO_3$ perovskite, the following convergence thresholds for geometry optimization were used: total energy variation smaller than 5.0×10^{-6} eV/atom in three successive self-consistent steps, 0.01 eV $Å^{-1}$ for maximum force, 0.02 GPa for maximum pressure, and 5×10^{-4} Å for maximum displacement. After reaching geometry convergence, the final average pressures obtained were 0.0039 GPa (LDA) and 0.0029 GPa (GGA). The symmetrized stress tensor components (also in GPa) were $\epsilon_{xx} = -0.012\,523(0.017\,894)$, $\epsilon_{yy} = -0.004\,411(-0.011\,349)$, $\epsilon_{zz} = 0.005\,229(-0.015\,136)$ for the LDA (GGA) computations (hydrostatic stress). In order to check for the accuracy of our results, we performed a GGA geometry optimization using a larger energy cutoff of 700 eV and a Monkhorst–Pack sampling of $6 \times 5 \times 7$ **k**-points. This refined calculation changed the lattice parameters by only 10^{-4} Å at most, and the unit-cell total energy decreased by just 0.3 eV.

Table 1. Lattice parameters and volume of the orthorhombic $CaSnO_3$ unit cell after geometry optimization within the LDA and GGA frameworks. The experimental data are from Zhao *et al* [8], and Mountstevens *et al* [9].

	a (Å)	b (Å)	c (Å)	V (Å)
LDA	5.4099	5.5887	7.7459	234.1919
GGA	5.6086	5.7978	8.0452	261.6101
Exp.	5.5142	5.6634	7.8816	246.1354

Following geometry optimization, the electronic band structure and the density of states (total and partial, and the relative contribution of each atom) were evaluated, as well as the optical absorption, using the same exchange–correlation functionals of the energy minimization, but replacing the ultrasoft pseudopotentials, in the case of optical absorption computations, by norm-conserved ones [24] with an energy cutoff of 900 eV. Such replacement is necessary due to limitations of the CASTEP code to take into account some contributions to the optical properties related to the use of ultrasoft pseudopotentials. The accuracy check mentioned in the previous paragraph was also accomplished for the electronic eigenenergies, that changed by 1 meV at most. This value is enough to assure the electronic structure convergence. Effective masses at the extrema of the valence and conduction bands were estimated by quadratic interpolation of the corresponding band curves following the scheme of Henriques *et al* [25, 26]. The optical absorption $\alpha(\omega)$ of orthorhombic $CaSnO_3$ was calculated following the same scheme of previous works [25–27].

The calculated optimized unit-cell parameters of $CaSnO_3$ orthorhombic are shown in table 1, together with experimental x-ray diffraction data [8, 9] for the sake of comparison. A good agreement with experimental data is obtained in general. The LDA underestimates the lattice parameters and unit-cell volume by -1.9% (a), -1.3% (b), -1.7% (c) and -4.9% (volume) in comparison to the experimental data. This result was already expected because the LDA tends to overbind the atoms in a crystal. On the other hand, the GGA functional usually predicts a larger unit cell by underestimating the interatomic forces. In the case of orthorhombic $CaSnO_3$, errors in the unit-cell lattice parameters when compared to the x-ray measurements were larger in magnitude than the values obtained using the LDA functional: $+1.7\%$, $+2.4\%$, $+2.1\%$ and $+6.3\%$ for a, b, c and unit-cell volume, respectively. Therefore, the LDA cell optimization gives better values for the orthorhombic $CaSnO_3$ lattice parameters. Indeed, the fact that the LDA yields a better equilibrium unit-cell size in comparison to experimental data is consistent with results obtained in the case of semiconductors [28–31]. Calculations of the pressure-dependent structural properties of $ScAlO_3$ perovskite performed by Magyari-Köpe *et al* [32] using total energy calculations estimated mean deviations of 0.4% and 6.5% for their LDA-calculated (2.0% and 7.9% for their GGA-calculated) average atomic radius and bulk modulus in comparison to experimental data [32]. Colson *et al* [33] carried out a first principles geometry optimization of the perovskite and hexagonal phases of $BaTiO_3$, finding that the LDA gives lattice parameters closer to experiment than the GGA. Although the LDA achieved a better geometry than the GGA, neither method presented a good agreement with experimental data for the lattice parameters (for example, their LDA calculation underestimates the a parameter of orthorhombic $BaTiO_3$ by 12%).

3. Band structure and optical absorption

Density functional theory (DFT) is a very useful tool to calculate the electronic ground-state properties of molecules and solids. The local density approximation (LDA) and the generalized

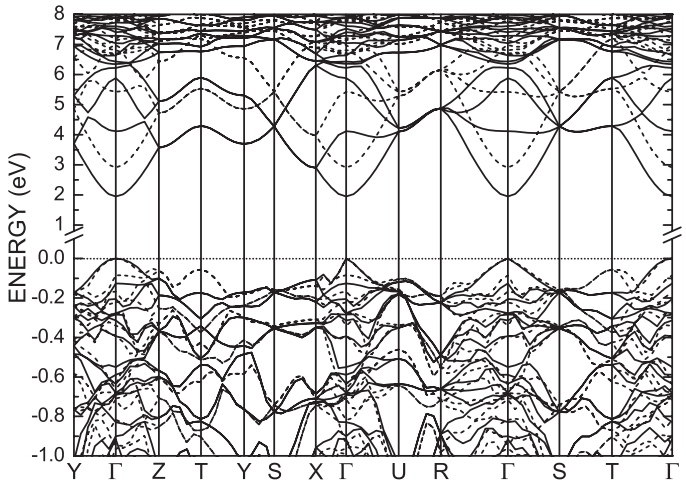

Figure 2. Electronic band structure near the Fermi level (chosen to be zero) for orthorhombic $CaSnO_3$ calculated within the LDA (dashed lines) and GGA (solid lines) frameworks.

gradient approximation (GGA) allow the prediction of structural and vibrational properties of many materials, but miss long-range correlations, failing to reproduce the ground-state energy surfaces of systems with van der Waals bonds or layered materials (for example, graphite) [34]. In DFT, a one-electron Schrödinger equation using an effective potential yields wavefunctions which produce a quite accurate ground-state electronic density, but with eigenvalues leading to inaccurate (underestimated) band gaps for semiconductors and insulators, with errors commonly of the order of or larger than 50% [35, 36]. In practice, the band gap energy and band structure are thus computed using many-body Green function techniques such as the GW method [37, 38]. In view of these facts, the results we present here on the band structure of orthorhombic $CaSnO_3$ should be considered with some caution.

The electronic band structure and partial density of states (PDOS) for orthorhombic $CaSnO_3$ were computed covering a wide range of energy levels, from -37.5 to 10 eV (0 eV being the Fermi level). In the full GGA band structure (not shown here), there are four energy bands at -37.5 eV, originating from Ca 3s levels (see figure 3), 12 bands near -18 eV with main contribution from Ca 3p states, and 12 bands between -17 and -15 eV whose main contributions stem from O 2s electrons. There are 36 uppermost valence bands from -7 to 0 eV, resulting mostly from O 2p orbitals, with smaller contributions from Sn 5s (between -7 and -5 eV) and Sn 5p (between -4 and -2 eV) levels. A total of 30 conduction bands were calculated, mixing contributions from calcium, oxygen, Sn 5s and Sn 5p states, as indicated in figure 3. For energies between 1.9 and 7 eV, the PDOS is small and is ruled by O 2p and Sn 5s. Above 7 eV, however, a very intense contribution from Ca 3d electrons emerges. Comparing the density of states predicted for $CaSnO_3$ with that calculated for orthorhombic $CaGeO_3$ [25], we note in the latter the absence of Ca 3d contributions to the lowermost conduction bands. This absence is not observed for β-$CaSiO_3$ [26]. It seems that the replacement of Si or Sn by Ge in some way precludes the formation of Ca 3d-related excited electronic levels, at least for the first 20 conduction bands of orthorhombic $CaGeO_3$.

The band structure for energies close to the main band gap is presented in figure 2, which depicts the GGA (solid) and LDA (dotted) results. For the lowest conduction bands (CBs) the LDA eigenenergies are practically 1 eV larger in comparison to the GGA calculations, leading to larger LDA band gaps. This huge difference is possibly related to the distinct structural

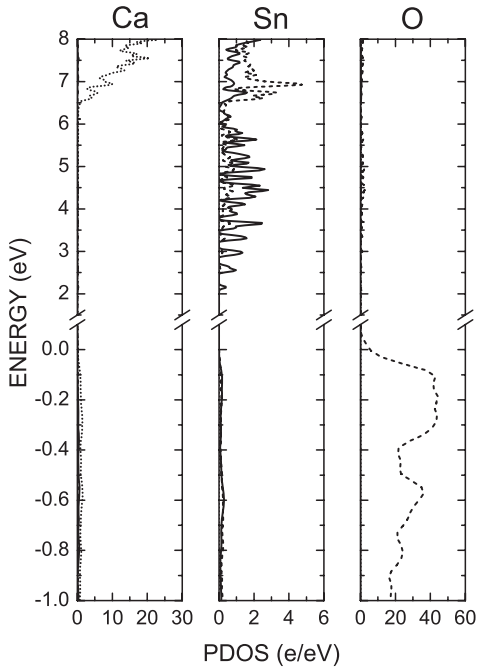

Figure 3. Partial density of states for Ca, Sn and O atoms in orthorhombic $CaSnO_3$. Contributions from s (solid lines), p (dashed lines) and d (dotted lines) orbitals.

parameters obtained after geometry optimization, as well as to the different electronic structure approximations embraced by each method. According to our results, orthorhombic $CaSnO_3$ has a direct band gap of 1.95 eV (GGA) and 2.92 eV (LDA), the LDA value being 1.5 times larger than the GGA energy gap. For the sake of comparison, results obtained for Si, Ge and GaAs using LDA and GGA approaches exhibit discrepancies of more than 100% between the energy gaps predicted by these levels of theory [39]. An indirect band gap 57 meV larger is observed between T at the valence band and Γ at the conduction band for both LDA and GGA data. We remember that due to the approximate nature of DFT functionals, theoretically calculated energy gaps are inaccurate and always smaller than experimental data [40]. Besides, experimental data will only be useful to cross-check the existence of direct or indirect gaps, and to estimate the theoretical error. Therefore, the smallest actual band gap of $CaSnO_3$ must be larger than 2.92 eV, and experimental data are necessary to allow for a direct comparison with the nature of the band gap (direct or indirect) predicted by theory. If we suppose that the real energy gap of this material is 30% [41]–70% [42, 43] larger than the LDA prediction (the latter error is observed for SnO_2 and In_2O_3), the actual $CaSnO_3$ energy gap is estimated to be in the 3.80–4.96 eV range. Consequently, the actual $CaSnO_3$ optical absorption should occur in the ultraviolet range of the electromagnetic spectrum.

The estimated $CaSnO_3$ energy band gap presented here is considerably smaller than: (i) the indirect energy gap $E^{\mathrm{LDA}}_{G(D\rightarrow Z)} = 4.95$ eV and $E^{\mathrm{GGA}}_{G(D\rightarrow Z)} = 5.07$ eV estimated recently [27] for $CaCO_3$ calcite (see also the calculations of Skinner *et al* [44]), in good agreement with the experimental value 6.0 ± 0.35 eV [45]; (ii) the indirect band gaps $E(\mathrm{Q} \rightarrow \Gamma) = 5.43$ eV and $E(\mathrm{B} \rightarrow \Gamma) = 5.44$ eV, and a direct gap $E(\Gamma \rightarrow \Gamma) = 5.52$ eV estimated for $CaSiO_3$ [26]. Orthorhombic $CaSnO_3$ energy gaps are comparable, on the other hand, to the two very close indirect (S → Γ) and direct (Γ → Γ) band gap energies of 1.68 eV (2.31 eV) and 1.75 eV

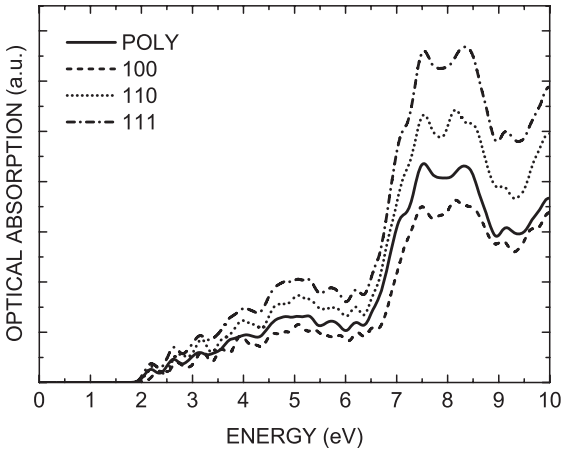

Figure 4. Orthorhombic $CaSnO_3$ optical absorption for polarized incident light and polycrystal sample.

Table 2. Carriers' effective masses of orthorhombic $CaSnO_3$ along some symmetry directions. All values are given in terms of the free electron mass m_0.

	LDA		GGA	
	Electron	Hole	Electron	Hole
$\Gamma \rightarrow X$	0.10	0.12	0.10	0.12
$\Gamma \rightarrow Y$	0.09	0.92	0.09	1.00
$\Gamma \rightarrow Z$	0.10	1.11	0.10	1.86
$\Gamma \rightarrow R$	0.10	0.43	0.10	0.49
$\Gamma \rightarrow S$	0.09	0.28	0.09	0.34
$\Gamma \rightarrow T$	0.09	1.22	0.10	1.25
$\Gamma \rightarrow U$	0.08	0.35	0.12	0.31

(2.41 eV) that were obtained within the GGA (LDA) for $CaGeO_3$ [25]. Consequently, the effect of the carbon replacement by higher atomic number elements of the same column in the periodic table, e.g., Si, Ge, and Sn, is to decrease the band gap energy, changing the character of the $CaXO_3$ (X = Ca, Si, Ge, Sn) material from insulating to semiconductor.

The semiconducting character of $CaSnO_3$ is reinforced by effective mass calculations, shown in table 2. It can be seen that the LDA masses are close to the GGA masses for both electrons and holes (closer for electrons). Hole effective masses are in general larger than electron masses and very anisotropic, varying between 0.12 m_0 and 1.86 m_0 at the Z point, where m_0 is the free space electron mass. Electron masses, on the other hand, are practically isotropic, being around 0.1 m_0. A similar behavior for the hole and electron effective masses (anisotropic hole masses, light and almost isotropic electron masses) was observed for wollastonite $CaSiO_3$ [26] and orthorhombic $CaGeO_3$ [25]. Thus, we can conclude from the small theoretical band gap and from the small effective masses that orthorhombic $CaSnO_3$ has the typical features of a semiconductor with a wide direct gap and parabolic conduction band, making this material interesting for optoelectronic applications.

Figure 4 shows the calculated optical absorption for $CaSnO_3$ considering incident light polarized along different crystal directions ([100], [110] and [111]) and polarized light incident on a polycrystal sample. We observe an increase of absorption intensity as the light polarizes along [111]. This is probably due to the almost complete alignment of oxygen and calcium

atoms when viewed along this direction. A Mulliken population analysis carried out for the GGA electronic structure reveals that the calcium atoms have a charge of 1.09 while each oxygen atom has −0.97 electrons (tin has a charge of 1.80). Bond analysis shows that Sn–O bonds have an electronic population between 0.35 and 0.38, while Ca–O bonds have an electronic population between 0.04 and 0.16, showing that Ca–O is more ionic in comparison to Sn–O. Stronger electronic dipole moment along [111], therefore, is expected, due to the alignment of Ca–O ionic bonds down this direction. As for the absorption in general, we identify two regimes, the first for energies below approximately 7 eV, and the second for energies above 7 eV. In the first range, absorption is weaker due to the scarcity of first-order transitions, occurring mainly from O 2p valence states to Sn 5s conduction states which host only a few electrons (see figure 3). When the energy reaches 7 eV, the transitions become mainly due to the interaction between O 2p valence states and Ca 3d conduction states. These Ca 3d states have more room for electrons and, consequently, allow for more transitions and more photonic absorption.

4. Conclusions

We have calculated the structural, electronic and optical absorption for orthorhombic $CaSnO_3$ through quantum *ab initio* calculations. The lattice parameters calculated after performing geometry optimization display a good agreement with experimental data. GGA overestimates the actual orthorhombic $CaSnO_3$ lattice parameters by 2.5% at most, while the LDA lattice parameters are underestimated by 2%. The smallest energy gap between the valence and band conductions is direct, corresponding for the LDA and GGA calculations to 1.95 and 2.92 eV, respectively. An indirect band gap 57 meV larger is predicted between T at the valence band and Γ at the conduction band for both LDA and GGA data. Assuming that the real energy gap is 30%–70% larger than the value predicted in the LDA calculation, the actual $CaSnO_3$ energy gap is estimated to be in the 3.80–4.96 eV range. Consequently, the actual $CaSnO_3$ optical absorption should occur in the ultraviolet range of the electromagnetic spectrum. Effective mass calculations reinforce the picture of orthorhombic $CaSnO_3$ as a semiconductor. LDA masses have values close to GGA masses for both electrons and holes (closer for electrons), with hole effective masses in general larger than electron masses and very anisotropic, while electron masses are practically isotropic and equal to 0.1 m_0. $CaSnO_3$, therefore, has features characteristic of a semiconductor with a wide direct gap and parabolic conduction band, exhibiting potential for optoelectronic applications. Calculated optical absorption for $CaSnO_3$ shows an increase of absorption intensity as the light polarizes along [111], probably due to the nearly perfect alignment of oxygen and calcium atoms when viewed along this direction. Two absorption regimes exist, the first for energies below approximately 7 eV, and the second for energies larger than 7 eV. In the first energy range, absorption is weaker due to the scarcity of first-order transitions, occurring mainly from O 2p valence states to Sn 5s conduction states with small PDOS. Increasing the photon energy beyond 7 eV leads to transitions between O 2p valence states and Ca 3d conduction states with large PDOS and, consequently, allows for more transitions and more photonic absorption in comparison to energies below 7 eV.

Acknowledgments

We thank the anonymous referees for the suggestions which helped us to improve the quality of this work. VNF, JAPC, and ELA are senior researchers from the Brazilian National Research Council CNPq, and would like to acknowledge the financial support received during the development of this work from the grants CNPq-CTENERG 504801/2004-0 and CNPq-Rede

NanoBioestruturas 555183/2005-0. JMH was sponsored by a graduate fellowship from the Brazilian National Research Council (CNPq) at the Physics Department of the Universidade Federal do Rio Grande do Norte.

References

[1] Kung L, Angel R J and Ross N L 2001 *Phys. Chem. Min.* **28** 35
[2] Sharma N, Shaju K M, Subb Rao G V and Chowdari B V R 2002 *Electrochem. Commun.* **4** 947
[3] Liu Z and Liu Y 2005 *Mater. Chem. Phys.* **93** 129
[4] Lu Z, Chen L, Tang Y and Li Y 2005 *J. Alloys Compounds* **387** L1
[5] Azad A-M, Shyan L L and Alim M A 1999 *J. Mater. Sci.* **34** 1175
[6] Mizoguchi H and Woodward P M 2004 *Chem. Mater.* **16** 5233
[7] Durand B and Loiseleur H 1978 *J. Appl. Crystallogr.* **11** 289
[8] Zhao J, Ross N L and Angel R J 2004 *Phys. Chem. Min.* **31** 299 and references therein
[9] Mountstevens E H, Attfield J P and Redfern S A T 2005 *J. Phys.: Condens. Matter* **15** 8315
[10] Hohenberg P and Kohn W 1964 *Phys. Rev.* **136** B864
[11] Kohn W and Sham L J 1965 *Phys. Rev.* **140** A1133
[12] Segall M D, Lindan P L D, Probert M J, Pickard C J, Hasnip P J, Clark S J and Payne M C 2002 *J. Phys.: Condens. Matter* **14** 2717
[13] Vanderbilt D 1990 *Phys. Rev.* B **41** 7892
[14] Koch W and Holthausen M C 2000 *A Chemist's Guide to Density Functional Theory* (Weinheim: Wiley–VCH) pp 65–91
[15] Ceperley D M and Alder B J 1980 *Phys. Rev. Lett.* **45** 566
[16] Perdew J P and Zunger A 1981 *Phys. Rev.* B **23** 5048
[17] Perdew J P, Burke K and Ernzerhof M 1996 *Phys. Rev. Lett.* **77** 3865
[18] Monkhorst H J and Pack J D 1976 *Phys. Rev.* B **13** 5188
[19] Pack J D and Monkhorst H J 1977 *Phys. Rev.* B **16** 1748
[20] Ackland G J 1998 *Phys. Rev. Lett.* **80** 2233
[21] Segall M D, Pickard C J, Shah R and Payne M C 1996 *Mol. Phys.* **89** 571
[22] Segall M D, Shah R, Pickard C J and Payne M C 1996 *Phys. Rev.* B **54** 16317
[23] Pfrommer B G, Cote M, Louie S G and Cohen M L 1997 *J. Comput. Phys.* **131** 133
[24] Lin J S, Qteish A, Payne M C and Heine V 1993 *Phys. Rev.* B **47** 4174
[25] Henriques J M, Caetano E W S, Freire V N, da Costa J A P and Albuquerque E L 2007 *Ab initio* structural, electronic and optical properties of orthorhombic $CaGeO_3$ *J. Solid State Chem.* at press
[26] Henriques J M, Caetano E W S, Freire V N, da Costa J A P and Albuquerque E L 2006 *Chem. Phys. Lett.* **427** 113
[27] Medeiros S K, Albuquerque E L, Maia F F Jr, Caetano E W S and Freire V N 2007 Band structure and carriers effective masses of $CaCO_3$ calcite *Solid State Chem.* submitted
[28] Vitos L, Johansson B, Kollár J and Skriver H L 2000 *Phys. Rev.* B **62** 10046
[29] Filippi C, Singh D J and Umrigar C J 1994 *Phys. Rev.* B **50** 14947
[30] Corso A D, Pasquarello A, Baldereschi A and Car R 1996 *Phys. Rev.* B **53** 1180
[31] Juan Y M, Kaxiras E and Gordon R G 1995 *Phys. Rev.* B **51** 9521
[32] Magyari-Köpe B, Vitos L and Kollár J 2001 *Phys. Rev.* B **63** 104111
[33] Colson T A, Spencer M J S and Yarovsky I 2005 *Comput. Mater. Sci.* **34** 157
[34] Rydberg H, Dion M, Jacobson N, Schrder E, Hyldgaard P, Simak S I, Langreth D C and Lundqvist B I 2003 *Phys. Rev. Lett.* **91** 126402
[35] Yin M T and Cohen M L 1982 *Phys. Rev.* B **26** 5668
[36] Hamann D R 1979 *Phys. Rev. Lett.* **42** 662
[37] Hedin L 1965 *Phys. Rev.* **139** A796
[38] Hedin L and Lundqvist S 1969 *Solid State Phys.* **23** 1
[39] Juan Y-M, Kaxiras E and Gordon R G 1995 *Phys. Rev.* B **51** 9521
[40] Gritsenko O V, Schipper P R and Baerends E J 1997 *J. Chem. Phys.* **107** 5007
[41] Godby R W, Schluter M and Sham L J 1983 *Phys. Rev. Lett.* **51** 1884
[42] Odaka H, Iwata S, Taga N, Ohnishi S, Kaneta Y and Shigesato Y 1997 *Japan. J. Appl. Phys.* **36** 5551
[43] Kilic C and Zunger A 2002 *Phys. Rev. Lett.* **88** 095501
[44] Skinner A J, LaFemina J P and Jansen H J F 1994 *Am. Mineral.* **79** 205
[45] Baer D R and Blanchard D L 1993 *Appl. Surf. Sci.* **72** 295